



Title	Two-temperature X-ray emission from the planetary nebula NGC 7293
Author(s)	Leahy, DA; Zhang, CY; Kwok, S
Citation	The Astrophysical Journal, 1994, v. 422 n. 1, p. 205-207
Issued Date	1994
URL	http://hdl.handle.net/10722/179681
Rights	Creative Commons: Attribution 3.0 Hong Kong License

TWO-TEMPERATURE X-RAY EMISSION FROM THE PLANETARY NEBULA NGC 7293

D. A. LEAHY,¹ C. Y. ZHANG,² AND SUN KWOK¹

Received 1993 July 26; accepted 1993 August 23

ABSTRACT

ROSAT PSPC observations of the planetary nebula NGC are reported here. This planetary nebula is here the first discovered to show clearly two components in its X-ray spectrum. A two-component model consisting of a blackbody and a Raymond-Smith thermal plasma is fitted to the observed *ROSAT* PSPC spectrum. This results in a temperature of $T_1 = 1.4 \times 10^5$ K for the blackbody component and a temperature $T_2 = 8.7 \times 10^6$ K for the hot plasma component, at a hydrogen column density $N_H = 1.4 \times 10^{20}$ cm⁻². The temperature of the blackbody component is consistent with the helium Zanstra temperature of the central star, indicating that it may be attributed to the photosphere of the central star. The high-temperature component is possibly from a corona around the central star, which may be related to a strong convection in the star. An alternative explanation is that the hot plasma resides in a hot bubble predicted by the interacting wind model. A lower limit of the electron density in the hot plasma is found to be ~ 10 cm⁻³.

Subject headings: planetary nebulae: individual (NGC 7293) — X-rays: ISM

1. INTRODUCTION

NGC 7293 (22^h26^m55^s, $-20^\circ 50' 15''$ [1950.0]) is a large and nearby planetary nebula (PN), also known as the Helix Nebula. It has a diameter of about 10' (Pottasch 1984) and an extinction of $c = 0.04$ (Kaler 1983). The hydrogen and He II Zanstra temperatures are estimated to be 110,000 and 113,000 K, respectively (Pottasch 1984). A spectroscopic effective temperature of the central star as derived by model fitting to the absorption line profiles is $\sim 90,000$ K (Mendez et al. 1988). A new method to determine the stellar core mass and luminosity (L_*) of planetary nebula central stars (PNCs) using distance-independent parameters from radio and infrared measurements found the core mass and luminosity of this PNCs to be $\sim 0.605 M_\odot$ and $\sim 100 L_\odot$, respectively (Zhang & Kwok 1993). These values lead to a distance estimate to NGC 7293 of 160 pc (Zhang 1993). Throughout this paper, we will adopt the distance of 160 pc.

Early detection of X-ray emission was made by the *Einstein* Observatory (Tarafdar & Apparao 1988) and the *EXOSAT* satellite (Apparao & Tarafdar 1989) for about 11 PNs. Apparao & Tarafdar (1989) found NGC 7293 to have an unabsorbed flux of $(6.9 \pm 1.9) \times 10^{-13}$ ergs cm⁻² s⁻¹. They estimated an X-ray luminosity (L_x) of 1.1×10^{30} ergs s⁻¹ at a distance of 116 pc. They suspected that this relatively low X-ray luminosity of NGC 7293 was due to an underestimated interstellar extinction. The X-ray emission from the detected PNs in the *Einstein* and *EXOSAT* observations was attributed to the photosphere of the PNCs by Apparao & Tarafdar (1989). They pointed out that X-rays from the PNCs would be visible when the nebula disperses or when the heavy elements in the PNCs atmosphere settle down.

Kreysing et al. (1993) have reported detection of X-ray emission from 6 PNs using *ROSAT* All Sky Survey, with an X-ray temperature of a few times 10^5 to 10^6 K. Five of the six PNs are claimed to have extended X-ray emission. Chu, Kwitter, &

Kaler (1993) have obtained *ROSAT* PSPC data of NGC 6853. They find that the emission from NGC 6853 is not extended, in contradiction to Kreysing et al.

The nature of the X-ray emission from planetary nebulae could not be fully understood through the early observations with *Einstein* and *EXOSAT*. Primarily owing to the faintness of planetary X-ray emission, it was impossible to obtain X-ray spectra of high enough quality from these previous X-ray satellites. Pointed observations with the *ROSAT* Position Sensitive Proportional Counter (PSPC) provide much improved sensitivity and can produce superior spectra for PNs. In this paper, we report observations of NGC 7293 with the *ROSAT* PSPC.

2. OBSERVATIONS

NGC 7293 was observed by the *ROSAT* PSPC counter during the third period of pointed observations (AO3). The energy response of the *ROSAT* X-ray telescope plus PSPC extends from approximately 0.1 to 2 keV. The PSPC at the focal plane provides an angular resolution of about 30' and a field of view of 2°. The spectral resolution is 40% (FWHM) at 1 keV. NGC 7293 was observed at the on-axis position for a total exposure time of 9.26 ks. We obtained a total of 345 net counts for this source.

The background-subtracted X-ray spectrum of NGC 7293 is shown in Figure 1. The net counts per channel are plotted against the channel energy. The 1σ error bars are also shown. The solid line histogram is the two-component model fit described below. This spectrum is characterized by a majority of photons in the energy range from 0.1 to 0.5 keV with a strong peak at about 0.12 keV and a low-energy cutoff determined by the detector. It is clear, however, that there is a broad secondary peak at about 0.8 keV.

3. RESULTS

The PSPC X-ray spectrum of NGC 7293 was fitted by several different spectral models. None of the single-component models can fit the observed spectrum. Two-component models, either blackbody plus Raymond-Smith (bb + RS), two-temperature blackbody (2T bb), or two-temperature Raymond-Smith (2T RS), are required to give satisfactory fits to the observed spectrum. The single-

¹ Department of Physics and Astronomy, University of Calgary, Calgary, Alberta, Canada T2N 1N4.

² Space Telescope Science Institute, 3700 San Martin Drive, Baltimore, MD 21218.

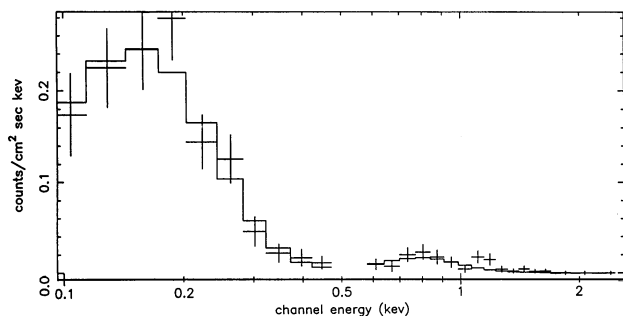


FIG. 1.—The *ROSAT* PSPC spectrum of NGC 7293 (data and folded model). Crosses are the observed net counts in each channel, with vertical bars indicating $\pm 1 \sigma$ errors. Solid line indicates the best-fit two-component (blackbody plus Raymond-Smith) model spectrum.

component models are rejected at high confidence. Thirty-one spectral channels were used in the fits.

The best fitting single-component model (bb) had a χ^2 per degree of freedom of 2.04 compared to the two-component models, which had values between 0.96 (bb + RS) and 1.03 (bb + bb). The best fitting single-component model (bb) had $kT = 0.011(\pm 0.001)$ keV, 1σ error, $N_{\text{H}} = 1.8(\pm 1.3) \times 10^{20} \text{ cm}^{-2}$, and normalization $A = 0.025$. The blackbody normalization A is defined as the bolometric flux, in particular, as luminosity in units of $10^{39} \text{ ergs s}^{-1}$ divided by distance in units of 10 kpc.

Results of the two-component model spectral fitting are as follows. The XSPEC package was used to perform the model fitting for the cases with blackbody components, since the PROS package did not go low enough in temperature. For the bb + RS model, the best-fit temperatures are $kT_1 = 0.011(\pm 0.001)$ keV ($T_1 = 1.3 \times 10^5$ K), normalization $A_1 = 0.026$ for the blackbody (bb) component; $kT_2 = 0.37(\pm 0.12)$ keV ($T_2 = 4.3 \times 10^6$ K), emission measure $\text{EM}_2 = 4.6 \times 10^9 \text{ cm}^{-5}$ for the Raymond-Smith (RS) component; and a column density of $N_{\text{H}} = 1.9(\pm 1.4) \times 10^{20} \text{ cm}^{-2}$. This best-fit model spectrum is shown in Figure 1 as the solid line. The high-temperature component dominates for > 0.25 keV and is significant down to 0.18 keV. The bb + bb model gave identical best-fit values for kT_1 and N_{H} , $A_1 = 0.023$, $A_2 = 2.0 \times 10^{-6}$, but the high-temperature component had a temperature $kT_2 = 0.15(\pm 0.03)$ keV. The best fitting 2T RS model was found using the PROS package (since XSPEC could not go low enough in temperature for the RS low-temperature component). The best fit had: $kT_1 = 0.012$ keV and emission measure $\text{EM}_1 = 5.5 \times 10^{14} \text{ cm}^{-5}$ (corresponding to a flux of $1.9 \times 10^{-13} \text{ ergs cm}^{-2} \text{ s}^{-1}$) for the low-temperature component; $kT_2 = 0.75$ keV and $\text{EM}_2 = 2.2 \times 10^9 \text{ cm}^{-5}$ (flux of $7.7 \times 10^{-14} \text{ ergs cm}^{-2} \text{ s}^{-1}$) for the high-temperature component; and a column density of $N_{\text{H}} = 1.4 \times 10^{20} \text{ cm}^{-2}$, with similar uncertainties as the 2T bb fit.

For purposes of the following discussion, we use values from the two-temperature blackbody plus the RS best-fit model since we feel this is most likely the correct physical description of the emission. We note that the flux values derived from the other two-component models are similar, and the uncertainties in the best-fit flux values are larger than the differences between the models. The observed X-ray fluxes are 2×10^{-13} and $8 \times 10^{-14} \text{ ergs cm}^{-2} \text{ s}^{-1}$, and the absorption-corrected X-ray fluxes are 4×10^{-11} and $9 \times 10^{-14} \text{ ergs cm}^{-2} \text{ s}^{-1}$, respectively, for the low-temperature and high-temperature com-

ponents. The unabsorbed X-ray luminosity in the range from 0.1 to 2 keV is therefore about $1.3 \times 10^{33} \text{ ergs s}^{-1}$ at the distance of 160 pc. Uncertainties in the estimated unabsorbed fluxes and luminosity come mainly from the uncertainties in the estimate of the interstellar extinction. The galactic hydrogen column density obtained from the best model fit of about $1.9 \times 10^{20} \text{ cm}^{-2}$ implies a color excess of $E(B-V) = 0.032$, or $c = 0.04$, using the conversion factor of $N_{\text{H}} = 5.8 \times 10^{21} E(B-V) \text{ cm}^{-2} \text{ mag}^{-1}$. This result is in good agreement with the value of $c = 0.04$ derived by Kaler (1983), using the Balmer decrement, the comparison of the radio continuum flux densities, and the colors of the central star. The X-ray luminosity of $1.1 \times 10^{30} \text{ ergs s}^{-1}$ obtained by Apparao & Tarafdar (1989) is much too low, mainly due to the zero interstellar extinction they adopted.

We have analyzed the spatial distribution separately for the low-energy (channels 7–40) and high-energy (channels 41–240) photons, using the PROS package. We divided the image into a set of annuli, with a width of each annulus of $15''$, and plotted the spatial profile of counts per pixel as a function of radius from the peak of the source (not shown). We shifted the center of the annuli to get the best possible centering on the X-ray source. The 50% encircled-energy radius is within about $30''$ for the low-energy component and $15''$ for the high-energy component. The on-axis radius of the circle containing 50% of the source counts is about $30''$ and $15''$, respectively, for a pure point source of soft and hard photons (from the point-spread function of Hasinger et al. 1992). Thus, neither of the two components is resolved by the *ROSAT* PSPC.

4. DISCUSSION

4.1. Low-Temperature Component

The low-energy component may be attributed to the photosphere of the PNCS, as the helium Zanstra temperature of $T_{\text{e}}(\text{He II}) = 1.13 \times 10^5$ K (Pottasch 1984) is consistent with our value of T_1 . Furthermore, this low-energy component is not spatially resolved by the *ROSAT* PSPC, indicating that the size of the source is less than $30''$. Suppose that the central star of NGC 7293 radiates like a blackbody; the angular radius of the star may be estimated from the observed X-ray flux as

$$\theta_* = \sqrt{\frac{F_x}{\pi \int_{\nu_1}^{\nu_2} B_{\nu}(T_*) d\nu}}, \quad (1)$$

where T_* is the central star temperature, F_x is the observed X-ray flux corrected for extinction over the frequency range from ν_1 to ν_2 , and B_{ν} the Planck function. If we take T_* as the helium Zanstra temperature of 1.13×10^5 K, and the unabsorbed X-ray flux of the low-energy component at Earth in § 3, we find from equation (1) that the angular radius of the low-energy X-ray emitting region is about 1.6×10^{-7} . This is not in conflict with the angular radius of the central star of 7.6×10^{-7} , estimated from the stellar bolometric luminosity $L_* = 100 L_{\odot}$ and the temperature of the star of 1.13×10^5 K. We conclude that the low-energy component of the X-ray emission is due to the stellar photosphere.

4.2. The High-Temperature Component

The X-ray luminosities, L_x , of NGC 246, 1360, 4361, 1535, 6853 and A36 derived from the *EXOSAT* results (Apparao & Tarafdar 1989) are to be in excess to the would-be X-ray luminosity implied by the X-ray Zanstra temperatures derived by the same authors (L_x can reach a few percent of L_*). This may

suggest that in addition to the stellar photosphere, contribution from an X-ray source related to a fast wind from the PNCS, a corona, and/or the PNCS being a binary system, where mass transfer plays a role, is needed. This “excess” X-ray emission would likely come from a hot plasma.

Our detection of the high-energy component in the X-ray spectrum of NGC 7293 clearly demonstrates the presence of a very hot plasma. It is possible that the central star might have developed a corona, which may be related to a strong convection in the star. An alternative explanation is the hot bubble predicted by the interacting wind model (Kwok 1982; Kahn 1983; Volk & Kwok 1985). Both can generate temperatures above 10^6 K. One way to distinguish between the two possibilities is to resolve the hot component spatially. The interacting stellar winds model predicts a hot bubble whose spatial extent is much larger than the stellar radius, while the corona should have a size which is comparable with the stellar photosphere.

The electron density of the high-energy component X-ray emitting region can be estimated from the emission measure obtained by the model fitting and the distance of the nebula, if the angular size is known. From our *ROSAT* PSPC data, the high-energy component is not resolved, giving an upper limit on angular radius of about $15''$. The lower limit for the electron density is

$$n_e = \sqrt{\frac{3(\text{EM})}{(n_p/n_e)\epsilon\theta_r^3 d}}, \quad (2)$$

where EM is the emission measure, (n_p/n_e) is 0.84 if the helium to hydrogen abundance ratio is 0.11, ϵ is the filling factor, θ_r is the angular radius of the emitting region, and d is the distance. Assuming $\epsilon = 0.6$, the lower limit of the electron density is 10 cm^{-3} . The true electron density in the region of the hot plasma can only be obtained accurately when the region is resolved. Thus, high spatial resolution imaging of the X-ray emission from PNs is highly desirable.

It is interesting to explore whether the observed temperature and fluxes of the high temperature component can be produced by the interacting winds model. Assuming that the hot bubble fills the entire inner region of the nebula, the temperature of the bubble is given by

$$T = \frac{\mu m_H \epsilon v^2}{9k}, \quad (3)$$

(Kahn 1983; Kwok & Leahy 1984), where μ ($= 0.62$) is the mean atomic weight of the gas, ϵ ($= 0.6$) is the assumed filling factor in the bubble, and v is the speed of the central star wind. For $v = 1000 \text{ km s}^{-1}$, $T \sim 0.43 \text{ keV}$, close to the observed value.

Assuming that the bubble is isobaric and has a uniform

density distribution, the density (ρ) in the bubble is

$$\rho = \frac{\dot{m}t}{\frac{4}{3}\pi R_s^3}, \quad (4)$$

where \dot{m} is the mass-loss rate of the central star wind, R_s is the radius of the bubble, and t is the dynamical age of the nebula. If we set the size of the bubble to equal to the radius of the nebula ($330''$), then a distance of 160 pc and an expansion velocity of 14 km s^{-1} (Acker et al. 1992) result in a dynamic age of 2×10^4 yr. This compares very well to the estimate of the central star of 10^4 yr from its position in the HR diagram. The predicted emission measure is

$$\text{EM} = \frac{4\pi}{3} n_e n_p \epsilon \frac{R_s^3}{4\pi D^2}. \quad (5)$$

An emission measure of $2.6 \times 10^9 \text{ cm}^{-5}$ is found for $\dot{m} = 10^{-8} M_\odot \text{ yr}^{-1}$.

The above calculations are based on the simple model of a uniform bubble completely filling the interior of the planetary nebular shell. If the X-ray emitting region is indeed confined to $15''$ as suggested by the data, then the density of the bubble should be higher. A mass-loss rate of $10^{-9} M_\odot \text{ yr}^{-1}$ will give an emission measure of $6 \times 10^{10} \text{ cm}^{-5}$. An observed size of $15''$ or less is a problem for the interacting winds model, since it would be difficult to obtain such a small filling factor for the $330''$ radius nebula.

5. CONCLUSION

An X-ray spectrum was obtained during pointed observations of NGC 7293 by the *ROSAT* PSPC counter. We have discovered the presence of two temperature components in the X-ray spectrum of a planetary nebula. A single-temperature spectral model cannot account for the observed spectrum of NGC 7293. A two-temperature component model is required. A model consisting of a blackbody component with a temperature of 130,000 K plus a hot plasma component with a temperature of 4.4×10^6 K gives a good fit to the observations. The low-temperature component is attributable to the photosphere of the central star: the temperature obtained from the X-ray spectrum is consistent with the helium Zanstra temperature of the central star, and the angular radius of the emitting region is consistent with that of the central star based on the bolometric luminosity, the temperature, and the distance of the central star. We propose that the X-ray emission of the high-temperature component originates from either a stellar corona or a hot bubble produced by the interaction between the fast wind from the central star and the slow wind of the remnant of the progenitor star.

This work is supported by the Natural Sciences and Engineering Research Council of Canada. C. Y. Z. acknowledges the support by NASA grant NAG 2-67.

REFERENCES

- Acker, A., Ochsenbein, F., Stenholm, B., Tylenda, R., Marcout, J., & Schohn, C. 1992, Strasbourg-ESO Catalogue of Galactic Planetary Nebula (Munich: ESO)
- Apparao, K. M. V., & Tarafdar, S. P. 1989, *ApJ*, 344, 826 (AT)
- Chu, Y.-H., Kwitter, K. B., & Kaler, J. B. 1993, *AJ*, in press
- Hasinger, G., Turner, T. J., George, I. M., & Boese, G. 1992, *Legacy*, 2, 77
- Kahn, F. D. 1983, in *IAU Symp. 103, Planetary Nebulae*, ed. D. R. Flower (Dordrecht: Reidel), 305
- Kaler, J. B. 1983, *ApJ*, 271, 188
- Kreysing, H. C., Diesch, C., Zweigle, J., Staubert, R., & Grewing, M. 1993, *A&A*, 264, 623
- Kwok, S. 1982, *ApJ*, 258, 280
- Kwok, S., & Leahy, D. A. 1984, *ApJ*, 283, 675
- Mendez, R. H., Kudritzki, R. P., Herrero, A., Husfeld, D., & Groth, H. G. 1988, *A&A*, 190, 113
- Pottasch, S. R. 1984, *Planetary Nebulae* (Dordrecht: Reidel)
- Tarafdar, S. P., & Apparao, K. M. V. 1988, *ApJ*, 327, 342
- Volk, K., & Kwok, S. 1985, *A&A*, 153, 79
- Zhang, C. Y. 1993, *ApJ*, 410, 239
- Zhang, C. Y., & Kwok, S. 1993, *ApJS*, in press